Phys. Status Solidi B **248**, No. 1, 117–122 (2011) / **DOI** 10.1002/pssb.201083982

physica status solidi b
www.pss-b.com
basic solid state physics

Modelling and testing of a foldable macrostructure exhibiting auxetic behaviour

Joseph N. Grima*[,1], Naveen Ravirala[2], Romina Galea[1], Brian Ellul[1], Daphne Attard[1], Ruben Gatt[1], Andrew Alderson[3], John Rasburn[3], and Kenneth E. Evans[3]

[1] Faculty of Science, University of Malta, Msida MSD 2080, Malta
[2] Institute for Materials Research and Innovation, University of Bolton, Deane Road, Bolton BL3 5AB, UK
[3] College of Engineering, Mathematics and Physical Sciences, Harrison Building, University of Exeter, Exeter, EX4 4QF, UK

Received 10 June 2010, revised 10 August 2010, accepted 12 August 2010
Published online 24 September 2010

Keywords auxetic behaviour, calix[4]arene, mechanical properties, Poisson's ratio

* Corresponding author: e-mail joseph.grima@um.edu.mt, Phone: +356 2340 2274 / + 356 7904 9865, Fax: +356 2133 0400

Auxetics exhibit the anomalous property of getting fatter rather than thinner when uniaxially stretched [negative Poisson's ratio (NPR)]. This paper presents an analytical model of a structure constructed from umbrella type sub-units which is predicted to exhibit this property together with the results of mechanical tests of a structure having this geometry. It is shown that such systems can exhibit negative on-axis Poisson's ratio of −1 which means that they maintain their aspect ratio, while Poisson's ratio becomes less negative for loading off-axis. It is also shown that this model can explain the sign and anisotropy of Poisson's ratio demonstrated by a molecular level system constructed from calix(4)arenes having the same geometry.

1 Introduction In recent years there has been an increased interest in materials and structures which exhibit the unusual property of becoming wider when stretched [1–35]. Such materials and structures, commonly known as auxetic [8], have a negative Poisson's ratio, NPR (conventional materials have a positive Poisson's ratio). In fact, the last two and a half decades have seen the design and development of various model structures [9–12] and materials which exhibit this property ranging from polyurethane foams [13–20] to nano- and microstructured polymers [21–33].

A particular class of polymers which has been predicted to exhibit NPR is the one constructed using calix(4)arene building blocks which are connected together as illustrated in Fig. 1 [29–31]. Force-field based simulations on various examples of such polymers have confirmed that they can exhibit NPR in the plane of the network. These networked polymers have the advantage that they can be constructed from available building blocks and have been designed to mimic the behaviour of an egg-rack macrostructure (see Fig. 1c).

This work reports an analytical model based on a simplified highly idealised system having the 'egg rack' geometry in an attempt to obtain a better understanding of the behaviour of this system when this is mechanically loaded in the plane of the structure. This is complemented by experimental work on the egg rack macrostructure, the results of which are then compared with the modelling predictions, and by a discussion of the earlier molecular modelling results in terms of the analytical model presented here.

2 Analytical modelling The proposed model is based on the geometry illustrated in Fig. 1 and will be aligned in space in such a way that the structure is aligned in the Ox_1–Ox_2 plane with one of the edges of the structure always aligned with the Ox_2 axis (see Fig. 2). In the model presented here, it will be assumed that the system is built using rods of infinite stiffness connected together through special three dimensional hinges which can be treated as two independent two dimensional 'hinges' where: (i) one hinge with stiffness k_θ allows hinging between the rods and an imaginary element parallel to the Ox_3 direction (θ hinging), and (ii) the second hinge with stiffness k_ϕ allows hinging between projections of the rods in the Ox_{12} planes (ϕ hinging) as illustrated in Fig. 2. The unit cell of this system is highlighted in bold lines in Fig. 2. Note that the θ hinges make the structure to behave as if it was constructed from umbrella-type sub units.

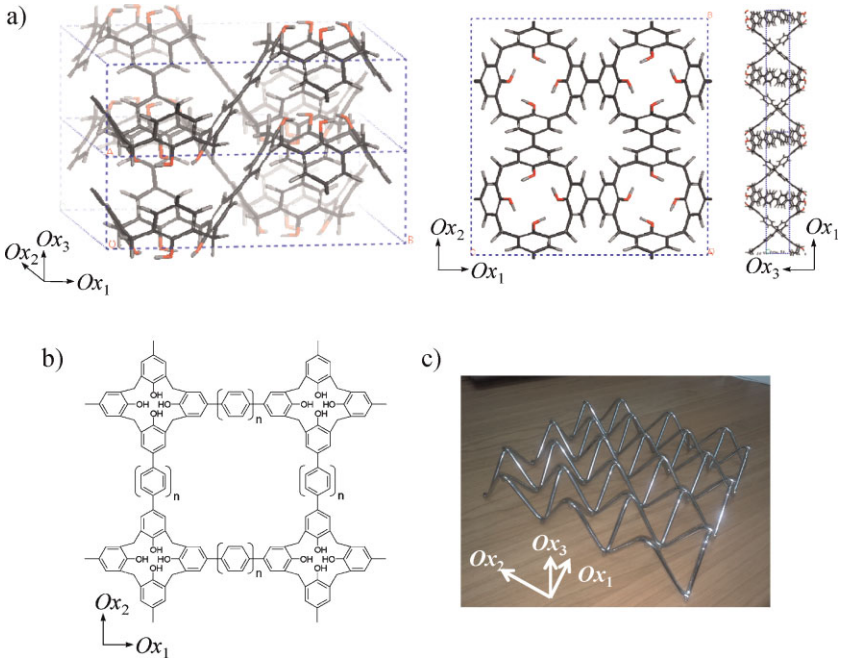

Figure 1 (online colour at: www.pss-b.com) (a, b) The molecular level system constructed from calix(4)arenes which is predicted to exhibit Poisson's ratios of −1; (c) the egg-rack macrostructure on which the molecular level honeycomb was designed.

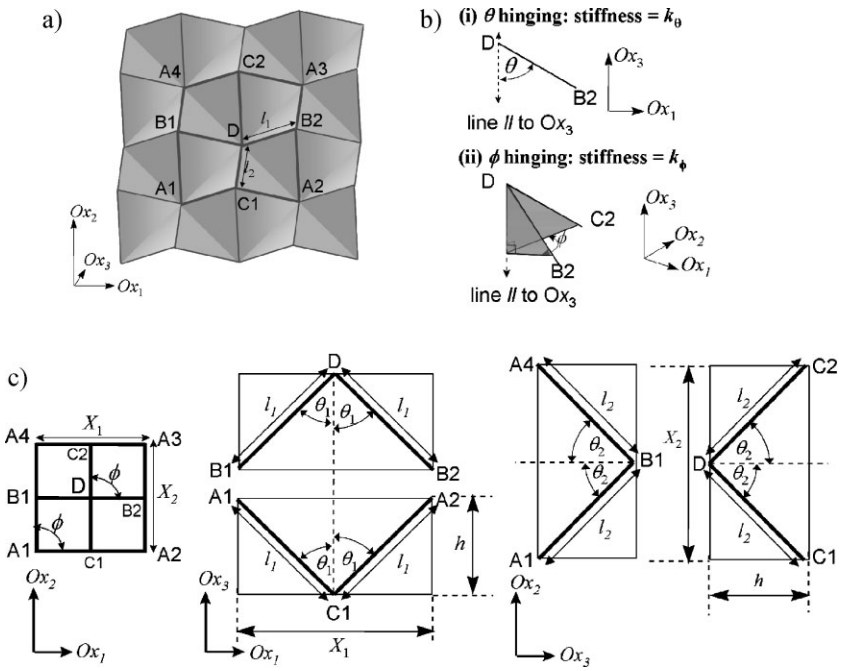

Figure 2 The definition of (a) the unit cell, (b) the hinges and (c) the geometric parameters. Note that one calyx represents four θ hinges and one ϕ hinge. (The shading in this illustration is only added to enhance the three dimensionality of the structure: the double calix structure is made up of rods, as illustrated by the bold lines.)

Referring to Fig. 2, the projections of the unit cell in the Ox_i direction ($i = 1,2,3$) are given by

$$X_1 = 2[l_1 \sin(\theta_1)], \tag{1a}$$

$$X_2 = 2[l_2 \sin(\theta_2)], \tag{1b}$$

$$X_3 = l_1 \cos(\theta_1) = l_2 \cos(\theta_2), \tag{1c}$$

where Eq. (1c) puts the constraint that

$$\theta_2 = \cos^{-1}\left(\frac{l_1}{l_2}\cos(\theta_1)\right). \tag{2}$$

If l_1 and l_2 are assumed to be constant (idealised hinging model) the size of the system is then dependent on a single variable. In this simplified model presented here, it will be

assumed that all rod lengths are of equal length l, *i.e.* it shall be assumed that $l_1 = l_2 = l$. Under such conditions, the structure is geometrically constrained to have $\theta_1 = \theta_2 = \theta$ (the single geometric variable) so that the cell projections are given by

$$X_1 = X_2 = 2l\sin(\theta), \quad X_3 = l\cos(\theta). \tag{3}$$

2.1 The on-axis Poisson's ratios and shear coupling coefficients for loading in the plane of the structure The Poisson's ratios in the $Ox_1{-}Ox_2$ plane are given by

$$\begin{aligned}\nu_{12} = (\nu_{21})^{-1} &= -\frac{\mathrm{d}\varepsilon_2}{\mathrm{d}\varepsilon_1} \\ &= -\left(\frac{1}{X_2}\frac{\mathrm{d}X_2}{\mathrm{d}\theta}\mathrm{d}\theta\right)\left(\frac{1}{X_1}\frac{\mathrm{d}X_1}{\mathrm{d}\theta}\mathrm{d}\theta\right)^{-1} \\ &= -\frac{X_1}{X_2}\frac{\mathrm{d}X_2}{\mathrm{d}\theta}\left(\frac{\mathrm{d}X_1}{\mathrm{d}\theta}\right)^{-1},\end{aligned} \tag{4}$$

where

$$\frac{\mathrm{d}X_1}{\mathrm{d}\theta} = \frac{\mathrm{d}X_2}{\mathrm{d}\theta} = 2l\cos(\theta). \tag{5}$$

Thus from these Eqs. (3)–(5), the Poisson's ratios for loading in the Ox_i ($i = 1,2$) directions are given by

$$\nu_{12} = \nu_{21} = -1, \tag{6}$$

which expression suggests that the on-axis Poisson's ratio of this idealised system is always equal to -1 irrespective of the length of rods or the angle 2θ between them. Such property is highly desirable as it means that this structure maintains its aspect ratio when it is uniaxially stretched or compressed on-axis.

Similarly, the Poisson's ratios in the $Ox_i{-}Ox_3$ planes ($i = 1,2$) for loading in the Ox_i ($i = 1,2$) directions are given by

$$\nu_{i3} = -\frac{\mathrm{d}\varepsilon_3}{\mathrm{d}\varepsilon_i} = -\frac{X_i}{X_3}\frac{\mathrm{d}X_3}{\mathrm{d}\theta}\left(\frac{\mathrm{d}X_i}{\mathrm{d}\theta}\right)^{-1} = +\tan^2(\theta), \tag{7}$$

which suggests that the Poisson's ratios ν_{i3} are always positive and are at a maximum for θ approaching 90°.

Loading of the structure in the through-thickness (Ox_3) direction will also lead to deformation through variation in θ and so in this case we also have

$$\nu_{i3} = \nu_{3i}^{-1}. \tag{8}$$

It is also clear that since uniaxial on-axis loading does not result in a change in the angle ϕ, then uniaxial on-axis loading will not result in a shear strain, and hence the shear coupling coefficients are equal to zero.

2.2 The Young's moduli Analytical expressions for the Young's moduli may be obtained from a conservation of energy approach. In particular, since for loading in the Ox_i directions ($i = 1,2$), the structure deforms solely through changes in the angles θ, then the strain energy per unit volume which accompanies a change in θ by $\mathrm{d}\theta$ is given by

$$\begin{aligned}U &= \frac{1}{2}E_i(\mathrm{d}\varepsilon_i)^2 = \frac{1}{2}E_i\left(\frac{1}{X_i}\frac{\mathrm{d}X_i}{\mathrm{d}\theta}\mathrm{d}\theta\right)^2 \\ &= \frac{1}{2}E_i\left(\frac{1}{X_i}\frac{\mathrm{d}X_i}{\mathrm{d}\theta}\right)^2(\mathrm{d}\theta)^2 = \frac{1}{2}E_i(\cot(\theta)\mathrm{d}\theta)^2,\end{aligned} \tag{9}$$

where this strain energy per unit volume U is related by the work done per unit cell W through

$$U = \frac{1}{V}W, \tag{10}$$

where V is the volume of the unit cell which is given by

$$V = X_1X_2X_3 = 4l^3\sin^2(\theta)\cos(\theta). \tag{11}$$

By noting that the number of θ hinges per unit cell is 16, then the work per unit cell required to change the value of θ by $\mathrm{d}\theta$ is given by

$$W = 16\left\{\frac{1}{2}k_\theta(\mathrm{d}\theta)^2\right\}, \tag{12}$$

and hence, from Eqs. (9)–(12), the Young's moduli for loading in the Ox_i ($i = 1,2$) directions are given by

$$E_1 = E_2 = \frac{4k_\theta}{l^3\cos^3(\theta)}. \tag{13}$$

Using a similar approach, the Young's modulus in the through-thickness direction is given by

$$E_3 = \frac{4k_\theta\cot(\theta)}{l^3\sin^3(\theta)}. \tag{14}$$

Examination of Eqs. (7), (8), (13) and (14) confirms that the model satisfies the thermodynamic requirement of a symmetric compliance matrix [34].

2.3 The shear modulus If a shear stress σ_{12} is applied, then the angles ϕ (and only ϕ) are expected to change. If we assume that each joint in the structure has one ϕ hinge (*i.e.* four ϕ hinges per unit cell), then the shear modulus may be derived in a similar method to the Young's modulus. Noting that in this case, the shear strain is equal to $\mathrm{d}\phi$, then the strain energy per unit volume, and the work done per unit cell are given respectively by

$$U = \frac{1}{2}G_{12}(\mathrm{d}\varepsilon_{12})^2 = \frac{1}{2}G_{12}(\mathrm{d}\phi)^2, \tag{15}$$

$$W = 4\left\{\frac{1}{2}k_\phi(\mathrm{d}\phi)^2\right\}, \tag{16}$$

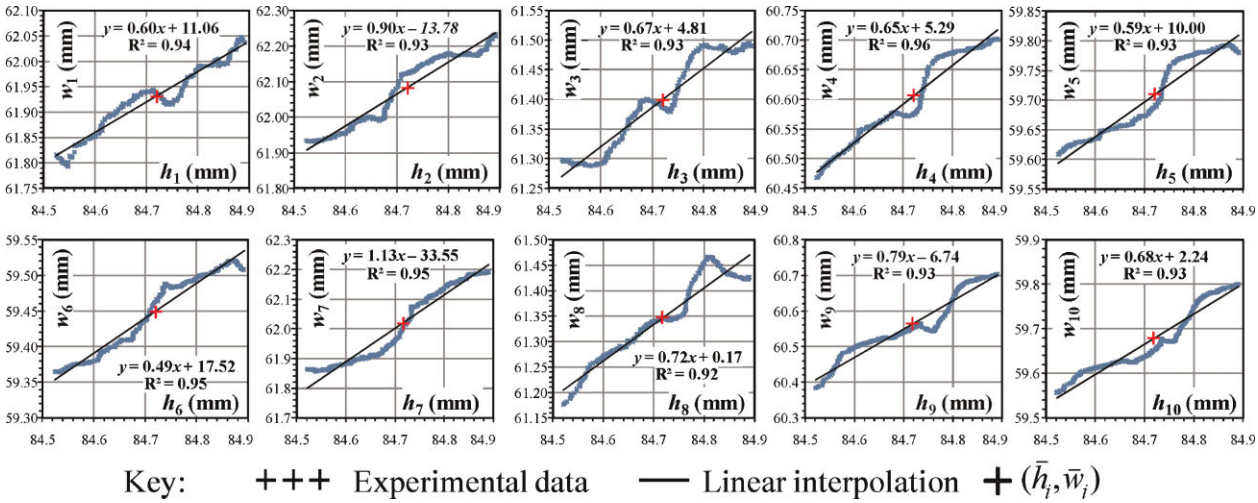

Figure 3 (online colour at: www.pss-b.com) Plots showing the experimentally obtained w_i *versus* h_i data from which the Poisson's ratio of the 'egg-rack' in Fig. 1c was calculated.

and hence from the principle of conservation of energy, Eqs. (10), (11), (15) and (16) we have

$$G_{12} = k_\phi \frac{1}{l^3 \sin^2(\theta)\cos(\theta)}. \tag{17}$$

3 Experimental work In an attempt to verify the suitability of the above model to reproduce the properties of such systems, the egg rack structure illustrated in Fig. 1c was mechanically tested under uniaxial compression using an Instron testing machine (Model No. 4303). Compression of the structure in the Ox_2 direction was carried out at a 2 mm/min strain rate to a maximum of 1% strain level. The axial and transverse strains, e_2 and e_1, respectively, were recorded using a MESSPHYSIK ME 46 videoextensometer. The videoextensometer software operates directly as a strain meter by determining the relative change in distance between markers placed along the length and width of the sample by tracking the change in the contrasts between markers as the compressive strain is applied. During the experiment, axial and transverse length data were recorded from which the axial and transverse strains were calculated. In this particular determination, two compression experiments were carried out, in each of which one measurement of the axial data (height direction, h, which shall be aligned to the global Ox_2 axis) was collected together with various transverse width data read at various sections along the length of the structure (width direction, w, which shall be aligned to the global Ox_1 axis). This methodology resulted in ten sets of the dimensions h_i and w_i ($i = 1, 2, \ldots 10$) between the markers in the height and width direction which were used to calculate ten estimates of the Poisson's ratio ν_i. Since it was observed that the (h_i, w_i) data could be adequately fitted to a linear curve $y = mx + c$, the Poisson's ratios were estimated as

$$\nu_{21,i} = -\frac{\varepsilon_1}{\varepsilon_2} \equiv -\frac{\mathrm{d}w}{\mathrm{d}h}\frac{\bar{h}_i}{\bar{w}_i},$$

where $\mathrm{d}w/\mathrm{d}h$ is the gradient obtained by the curve fitting exercise and $(\bar{h}_i, \bar{w}_i)$ are the averages of the (h_i, w_i) data (Fig. 3).

The results of the ten Poisson's ratios obtained using this procedure together with the r^2 values for the curve fitting to the $y = mx + c$ are shown in Table 1. These results clearly show that the Poisson's ratio of this structure is negative and equal to -1, this being in good agreement with the derived expression for the on-axis Poisson's ratio above.

4 Discussion and conclusion The expressions derived above and results of the experimental work confirm the potential of these systems to exhibit auxetic behaviour. They can also provide valuable information on the strengths and limitations of this geometry. In particular, the model highlights that whilst the in-plane on-axis Poisson's ratio of this idealised systems is always negative and equal to -1 meaning the structure maintains it aspect ratio, the out of

Table 1 The measured Poisson's ratios and R^2 values for the different tests and measurements performed. Note that the average Poisson's ratio from these results is equal to -0.93.

measurement	1	2	3	4	5	6	7	8	9	10	average
ν_{21}	−0.82	−1.22	−0.92	−0.91	−0.83	−0.71	−1.54	−1.00	−1.11	−0.96	−1.00
R^2	0.94	0.93	0.93	0.96	0.93	0.95	0.95	0.92	0.93	0.93	

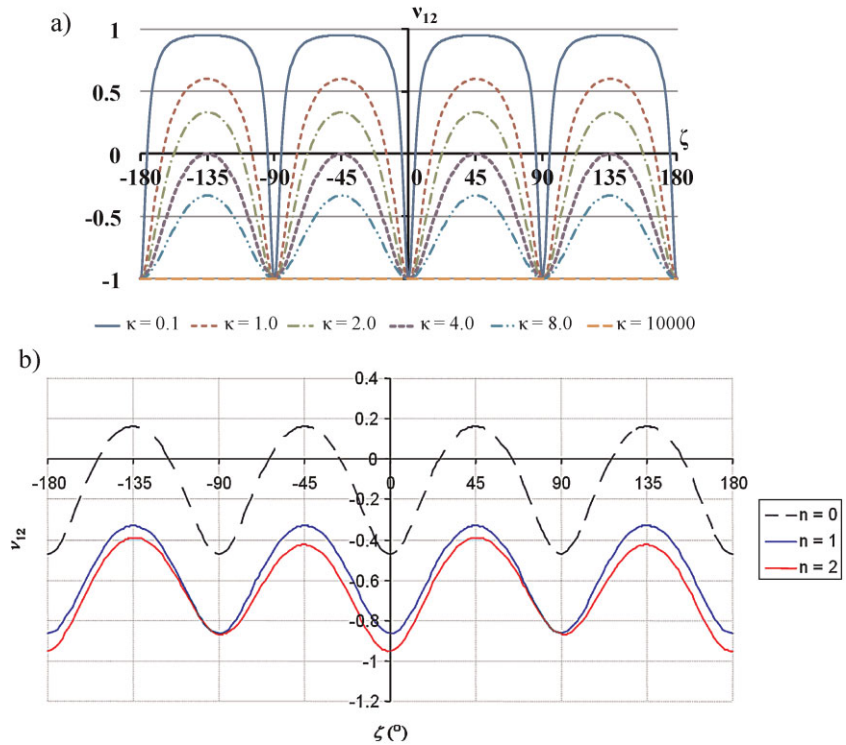

Figure 4 (online colour at: www.pss-b.com) (a) The in-plane off-axis Poisson's ratios for loading at an angle ζ to the Ox_1 direction with an angle $\theta = 45^\circ$, (b) the predicted in-plane off-axis Poisson's ratios for the molecular level networks. Note that these properties were calculated using the derived/simulated on-axis Poisson's ratios and moduli which were transformed using standard axis transformation techniques [36].

plane Poisson's ratio is always positive and can assume very high positive values (it tends to $+\infty$ as $\theta \to 90^o$). Furthermore, given the on-axis mechanical properties, the off-axis properties may be calculated using standard off-axis transformation techniques [35]. Typical plots of the off-axis Poisson's ratio in the plane of the structure are shown in Fig. 4 which clearly suggest that maximum auxeticity of a value -1 occurs for loading on-axis with the most non-auxetic behaviour occurring at $\pm 45^o$ off-axis where the Poisson's ratios are equal to

$$[\nu_{12}]_{\zeta=\pm 45^o} = -\frac{\kappa\cos^2(\theta) - 4\sin^2(\theta)}{\kappa\cos^2(\theta) + 4\sin^2(\theta)}, \tag{18}$$

where

$$\kappa = \frac{k_\phi}{k_\theta}. \tag{19}$$

This means that in the region $0 < \theta < 90^o$, the in-plane Poisson's ratios will be negative for all directions of in-plane loading if

$$\kappa\cos^2(\theta) - 4\sin^2(\theta) > 0, \tag{20}$$

i.e.

$$\kappa > 4\tan^2(\theta) \Rightarrow k_\phi > 4\tan^2(\theta)k_\theta, \tag{21}$$

thus suggesting that to maximise the auxeticity, the systems must be designed so as to maximise the θ hinging.

It is also interesting to note that the profiles of the off-axis plots obtained in Fig. 4 are very similar to the ones that had been obtained following molecular force-field based studies on the calix-4-arene networks. In fact, referring to Figs. 1 and 4, when systems with $n = 0$, 1 and 2 are modelled using the PCFF force-field, it was shown that the profile of the off-axis Poisson's ratio in the plane of the structures will also exhibit maximum auxeticity in the directions which correspond to on-axis in our analytical model and minimum auxeticity (if any) for loading at 45° off-axis, this being in full accordance with the predictions from the analytical model. Furthermore, it should be noted that as the number of phenyl rings between the calixes increases, the on-axis Poisson's ratio tend to the value of -1 predicted by the analytical model and the experimental work. In this respect it should be noted that in such molecular-level systems, deviations from the idealised behaviour should be expected as the model presented here only assumes deformations involving changes in angles between the rods (idealised hinging model) while the real systems are likely to deform through various modes of deformation. Furthermore, as explained elsewhere [29–31], the geometry of the polycalix molecular networks deviates slightly from the geometry of the model structure presented here, the deviations being most noticeable in the systems with short polyphenyl chains (*e.g.*

$n = 0$). Nevertheless, despite all these limitations, the agreement between the analytical model presented here and the behaviour of the more complex molecular level networks is remarkable.

The analytical model presented here assumes deformation occurs through hinging. In the mechanical model tested here it is possible the structure deforms predominantly through flexure of the ribs. Flexing and hinging modes of deformation have been found to be described by the same Poisson's ratio expressions in, *e.g.* hexagonal honeycomb structures [36, 37] and we expect this will be the case for the system considered here. To identify such deformation mechanisms, more detailed tests, or, finite elements simulations [38] will be required. In this respect, it should be noted that a more generic model would also incorporate other modes of deformations such as flexure and/or stretching of the ribs [38]. A fully generalised model should also allow the length of the ribs along the Ox_1 and Ox_2 directions to be different to each other.

Nevertheless, the model presented here has the advantage of simplicity. It is thus easy to interpret and can present valuable information to experimentalists who may wish to design auxetic materials and structures based on the topology presented here.

Acknowledgements The financial support of the UK AUXETNET network funded by the EPSRC, the University of Exeter as well as that of the Maltese government through the scholarship grant awarded to DA is gratefully acknowledged.

References

[1] K. W. Wojciechowski, Phys. Lett. A **137**, 305 (1989).
[2] C. Remillat, F. Scarpa, and K. W. Wojciechowski, Phys. Status Solidi B **246**, 2007 (2009).
[3] J. N. Grima and K. W. Wojciechowski, Phys. Status Solidi B **245**, 2369 (2008).
[4] C. W. Smith and K. W. Wojciechowski, Phys. Status Solidi B **245**, 486 (2008).
[5] K. W. Wojciechowski, A. Alderson, K. L. Alderson, B. Maruszewski, and F. Scarpa, Phys. Status Solidi B **244**, 813 (2007).
[6] K. W. Wojciechowski, A. Alderson, A. Braka, and K. L. Alderson, Phys. Status Solidi B **242**, 497 (2005).
[7] J. J. Williams, C. W. Smith, K. E. Evans, Z. A. D. Lethbridge, and R. I. Walton, Chem. Mater. **19**, 2423 (2007).
[8] K. E. Evans, M. A. Nkansah, I. J. Hutchinson, and S. C. Rogers, Nature **353**, 6340 (1991).
[9] R. F. Almgren, J. Elasticity **15**, 427 (1985).
[10] S. V. Dmitriev, T. Shigenari, and K. Abe, J. Phys. Soc. Jpn. **70**, 1431 (2001).
[11] K. W. Wojciechowski, J. Phys. A **36**, 11765 (2003).
[12] R. Lakes and K. W. Wojciechowski, Phys. Status Solidi B **245**, 545 (2008).
[13] R. S. Lakes, Science **235**, 1038 (1987).
[14] R. S. Lakes and K. E. Elms, J. Composite Mater. **27**, 1193 (1993).
[15] J. B. Choi and R. S. Lakes, Cell. Polym. **10**, 205 (1991).
[16] J. B. Choi and R. S. Lakes, Int. J. Mech. Sci. **37**, 51 (1995).
[17] K. E. Evans, M. A. Nkansah, and I. J. Hutchinson, Acta Metall. Mater. **42**, 1289 (1994).
[18] F. Scarpa, L. G. Ciffo, and Y. R. Yates, Smart Mater. Struct. **13**, 49 (2004).
[19] J. N. Grima, R. Gatt, N. Ravirala, A. Alderson, and K. E. Evans, Mater. Sci. Eng., A **423**, 214 (2006).
[20] J. N. Grima, D. Attard, R. Gatt, and R. N. Cassar, Adv. Eng. Mater. **11**, 533 (2009).
[21] C. He, P. Liu, and A. C. Griffin, Macromolecules **31**, 3145 (1998).
[22] C. He, P. Liu, A. C. Griffin, C. W. Smith, and K. E. Evans, Macromol. Chem. Phys. **206**, 233 (2005).
[23] W. Ren, P. J. McMullan, and A. C. Griffin, Phys. Status Solidi B **246**, 2124 (2009).
[24] K. E. Evans and B. D. Caddock, J. Phys. D **22**, 1883 (1989).
[25] A. P. Pickles, R. S. Webber, K. L. Alderson, P. J. Neale, and K. E. Evans, J. Mater. Sci. **30**, 4059 (1995).
[26] N. Ravirala, A. Alderson, K. L. Alderson, and P. J. Davies, Polym. Eng. Sci. **45**, 517 (2005).
[27] V. R. Simkins, N. Ravirala, P. J. Davies, A. Alderson, and K. L. Alderson, Phys. Status Solidi B **245**, 598 (2008).
[28] K. L. Alderson, A. Alderson, P. J. Davies, G. Smart, N. Ravirala, and G. Simkins, J. Mater. Sci. **42**, 7991 (2007).
[29] J. N. Grima, J. J. Williams, and K. E. Evans, Chem. Commun. 4065 (2005).
[30] J. N. Grima, J. J. Williams, R. Gatt, and K. E. Evans, Mol. Simul. **31**, 907 (2005).
[31] J. N. Grima, D. Attard, R. Cassar, L. Farrugia, L. Trapani, and R. Gatt, Mol. Simul. **34**, 1149 (2008).
[32] L. J. Hall, V. R. Coluci, D. S. Galvão, M. E. Kozlov, M. Zhang, S. O. Dantas, and R. H. Baughman, Science **320**, 504 (2008).
[33] V. R. Coluci, L. J. Hall, M. E. Kozlov, M. Zhang, S. O. Dantas, D. S. Galvão, and R. H. Baughman, Phys. Rev. B **78**, 115408 (2008).
[34] B. M. Lempriere, Am. Inst. Aeronaut. Astronaut. J. **6**, 2226 (1968).
[35] J. F. Nye, Physical Properties of Crystals (Oxford University Press, USA, 1957).
[36] L. J. Gibson, M. F. Ashby, G. S. Schajer, and C. I. Robertson, Proc. R. Soc. Lond. A **382**, 25 (1982).
[37] I. G. Masters and K. E. Evans, Composite Struct. **35**, 403 (1996).
[38] R. Galea, M.Sc. Thesis, University of Malta, Malta, 2010.

